PERGAMON

International Journal of Multiphase Flow 25 (1999) 1161–1180

International Journal of Multiphase Flow

www.elsevier.com/locate/ijmulflow

Drop formation at the surface of plane turbulent liquid jets in still gases

K.A. Sallam, Z. Dai, G.M. Faeth*

Department of Aerospace Engineering, The University of Michigan, Ann Arbor, MI 48109-2140, USA

Received 28 September 1998; received in revised form 8 April 1999

The authors dedicate the present paper to Gad Hetsroni as part of this Festschrift. We also wish to extend our best wishes to him on the occasion of this milestone in his career.

Abstract

An experimental study of drop formation at the free surface of plane turbulent jets in gases (i.e., turbulent primary breakup) is described. Test conditions consisted of fully-developed turbulent plane water jets injected into still air at standard temperature and pressure with Reynolds numbers of 91,000–424,000, Weber numbers of 13,000–151,000 and Ohnesorge numbers of 0.0009–0.0012. Pulsed shadowgraphy was used to measure mean liquid surface velocities, mean and fluctuating drop velocities after primary breakup, drop sizes after primary breakup and the location of the onset of primary breakup. Drop velocities were related to the average streamwise velocity in a relatively simple manner, while drop size properties could be related to earlier findings for turbulent primary breakup of round liquid jets in still gases using hydraulic diameter concepts.

Keywords: Atomization; Drop breakup; Sprays; Turbulence

1. Introduction

Drop formation along the free surface of plane turbulent liquid jets in gases was studied experimentally. This process, which is frequently called turbulent primary breakup, is important for spray formation for a variety of industrial and natural phenomena, e.g., liquid

* Corresponding author. Tel.: +1-734-764-7202; fax: +1-734-936-0106.
E-mail address: gmfaeth@umich.edu (G.M. Faeth)

0301-9322/99/$ - see front matter
PII: S0301-9322(99)00042-7

jets, chutes, spillways, plunge pools, hydraulic jumps, bow sheets and open waterwaves, among others (Gad-el-Hak, 1981; Townson, 1988; Ervine and Falvey, 1987). The objective of the present investigation was to extend recent studies of turbulent primary breakup for round liquid jets in still gases due to Wu et al. (1992, 1995), Wu and Faeth (1993, 1995) to consider plane liquid jets using similar methods.

Processes of turbulent primary breakup were identified during early flow visualization studies of de Juhasz et al. (1932), Lee and Spencer (1933a, 1993b). Subsequent studies of Schweitzer (1937), Grant and Middleman (1966), Phinney (1973), McCarthy and Malloy (1974) confirmed that liquid turbulence properties affected jet stability, the onset of breakup and spray quality after breakup. Finally, Hoyt and Taylor (1977a, 1977b) demonstrated that aerodynamic effects were generally of secondary importance for turbulent primary breakup in air at standard temperature and pressure (STP), by showing that liquid surface properties for coflowing and counterflowing air were essentially the same.

Subsequent work in this laboratory considered the liquid surface and turbulent primary breakup properties of round turbulent free jets (Ruff et al., 1989, 1991, 1992; Tseng et al., 1992; Wu et al., 1992, 1995; Wu and Faeth, 1993, 1995) and for plane turbulent wall jets (Dai et al., 1997, 1998a) in still gases. Pulsed shadowgraphy and holography were used to observe both liquid surface properties and drop properties after turbulent primary breakup. The results showed that aerodynamic effects were small for liquids injected into light gases (air, etc.) at STP, except far from the injector where primary and secondary breakup occur at comparable times and tend to merge (Wu and Faeth, 1993). Drop properties could also be related to liquid turbulence properties using phenomenological theories to yield successful correlations for properties at the onset and end of turbulent primary breakup and the evolution of drop sizes after turbulent primary breakup with distance along the surface. Differences between the turbulent primary breakup properties of round free jets and plane wall jets were observed, which raises questions about the role of the geometry change in causing these differences that have not yet been resolved.

In view of current understanding about turbulent primary breakup, the objective of the present investigation was to complete experimental observations of turbulent primary breakup of plane liquid jets in still gases and to interpret the new measurements using phenomenological theories. These results are of interest due to direct applications to spray formation in practical plane flows such as bow sheets, as well as for helping to resolve effects of flow curvature on primary breakup properties. The present experiments were carried out using large aspect ratio turbulent annular water jets (to approximate plane water jets) in still air at STP. The flows were observed using pulsed shadowgraphy, while phenomenological analysis was used to help interpret and correlate the measurements. A preliminary report of the study, emphasizing experimental methods, flow visualization and liquid surface properties, was presented by Dai et al. (1998b). The present paper provides more extensive results about drop properties after turbulent primary breakup along plane water jets in still air.

The article begins with consideration of experimental methods. Results are then described treating flow visualization, liquid surface velocities, drop size and velocity distributions, drop velocity moments, properties of the onset of breakup and moments of drop sizes after breakup, in turn.

2. Experimental

2.1. Apparatus

Pressure injection was used to feed water from a cylindrical storage chamber through an annular nozzle directed vertically downward at its bottom. The storage chamber had an inside diameter and length of 190 and 305 mm, respectively. The annular nozzle had a 50 mm inner diameter with annulus widths, b, of 3.55 and 6.75 mm to yield annular liquid jets, having aspect ratios greater than 23 to approximate plane free jets. The nozzle passages had rounded entries (radii of curvature of 1.5 times the annulus width) followed by annular passages having length/hydraulic diameter ratios greater than 40 : 1 both to avoid developing cavitating flows and to insure fully-developed turbulent flow at the jet exit (Ruff et al., 1992; Wu et al., 1995). The core of the annulus was well ventilated to prevent collapse of the annulus sheet after leaving the injector.

Liquid was placed in the storage chamber through a port with premature outflow prevented by an annular cork at the nozzle exit. The liquid was forced through the nozzle, ejecting the cork, by admitting high-pressure air to the top of the storage chamber through a solenoid valve. A baffle was used to control mixing between the air and the test liquid. The high-pressure air was stored in an accumulator having a volume of 0.12 m^3 on the upstream side of the solenoid valve, with provision for accumulator air pressures up to 1.9 MPa. The test liquid was captured in a baffled tub. The nozzle assembly could be traversed vertically with an accuracy of 0.5 mm using a linear bearing system, in order to accommodate rigidly-mounted optical instrumentation.

Injection times of 100–400 ms were long compared to flow development times of 6–70 ns. Present optical measurements required less than 0.1 ms for triggering and data acquisition, which did not impose any limitations on flow times. Jet velocities were calibrated in terms of the nozzle pressure drop by measuring liquid surface velocities using double pulse shadowgraphs as discussed later.

2.2. Instrumentation

Instrumentation consisted of single- and double-pulse shadowgraphy using an arrangement similar to Dai et al. (1998a). Two frequency-doubled YAG lasers were used for light sources. These lasers could be controlled to provide pulse separations as small as 100 ns. The shadowgraphs were recorded using a 100×125 mm film format with magnification of these records of 2–7. The photographs were obtained with an open camera shutter under darkroom conditions so that the 7 ns laser pulse duration controlled the exposure time and was sufficiently short to stop liquid surface motion. Different laser pulse strengths resolved directional ambiguity. The images were measured by mounting them on a two-dimensional traversing system having a 1 μm resolution that was viewed by a video camera, and reduced using an image analysis program developed by Ruff et al. (1991). The overall arrangement allowed drops as small as 5 μm diameter to be observed and as small as 10 μm diameter to be measured with 10% accuracy.

Data was reduced as described by Wu et al. (1992). Irregular drops were assumed to be

ellipsoids and were assigned diameters equal to the diameter of the sphere having the same volume as the ellipsoid. Except for effects of this definition of drop diameters, which are difficult to quantify, experimental uncertainties for drop diameters larger than 10 μm are less than 10%, increasing inversely to the drop diameter for smaller sized drops. Measurements of SMD, the Sauter mean diameter, were obtained by summing over 20–400 objects at each condition to obtain experimental uncertainties (95% confidence) less than 22%, mainly dominated by sampling limitations when relatively few drops appeared on particular shadowgraph photographs.

Measurements of liquid surface velocities were based on the motion of particular points along ligaments and other surface irregularities while summing over 40–200 points to find average surface velocities with experimental uncertainties (95% confidence) less than 10%, mainly dominated by sampling limitations. Mean and fluctuating drop velocities after primary breakup were measured in the same way to yield experimental uncertainties (95% confidence), as follows: mean streamwise velocity less than 10%, mean cross stream velocity less than 30% and rms fluctuating streamwise and cross stream velocities less than 20%. Corresponding measurements of mean and fluctuating velocities at various drop sizes, to find drop velocity distributions, also had experimental uncertainties (95% confidence) of less than 30% due to sampling limitations

Measurements of the location of the onset of turbulent primary breakup were obtained as the average of 15–30 experiments with relatively large experimental uncertainties (95% confidence) of less than 25% due to sampling limitations.

2.3. Test conditions

Present tests were limited to water injected into still air, however, past work concerning round free jets and plane wall jets in still air has shown that effects of variations of liquid and gas properties can be treated effectively by the dimensionless parameters used to summarize the present test results (Wu et al., 1992; Wu and Faeth, 1993, 1995; Dai et al., 1998a, 1998b). The test conditions used for the present investigation are summarized in Table 1. Hydraulic diameters, d_h, were approximated as $2b$, yielding values of 7.1 and 13.5 mm. Mean velocities at the jet exit, $\overline{u}_0$, were in the range 11.5–28.2 m/s. These parameter ranges yield the ranges of the

Table 1
Summary of test conditions[a]

Parameter	Formula	Range
b (mm)		3.55–6.75
$\overline{u}_0$ (m/s)		11.5–28.2
Re_{Ld}	$\rho_L \overline{u}_0 d_h/\mu_L$	91,000–424,000
We_{Ld}	$\rho_L \overline{u}_0^2 d_h/\sigma$	13,000–151,000
Oh_{Ld}	$\mu_L/(\rho_L d_h \sigma)^{1/2}$	0.000916–0.00126

[a] Plane water jet in air at 100 kPa and 300 ± 2 K. Properties of air: $\rho_G = 1.16$ kg/m^3 and $\mu_G = 18.5 \times 10^{-6}$ Ns/m^2. Properties of water: $\rho_L = 997$ kg/m^3, $\mu_L = 894 \times 10^{-6}$ Ns/m^2 and $\sigma = 0.0708$ N/m. Hydraulic diameters approximated as $2b$.

Reynolds number, Re_{Ld}, Weber number, We_{Ld} and Ohnesorge number, Oh_{Ld}, summarized in the table. The definitions of Re_{Ld}, We_{Ld} and Oh_{Ld} are also summarized in the table, where ρ and μ are the density and molecular viscosity while the subscripts L and G denote liquid and gas properties, respectively, and σ is the surface tension. The present Reynolds number range, combined with the relatively large length-to-hydraulic diameter ratios of the injector passage, is sufficiently high to ensure fully developed turbulent pipe flow at the jet exit (Wu et al., 1995). At the same time, the present rather small Ohnesorge numbers imply relatively small direct effects of liquid viscosity on turbulent primary breakup.

3. Results and discussion

3.1. Flow visualization

Shadowgraphs of the flow at various streamwise distances, x, from the jet exit are illustrated in Figs. 1 and 2. These results are for an annulus width of 6.75 mm with mean jet exit velocities of 15.8 and 28.2 m/s, for results illustrated in Figs. 1 and 2, respectively. The direction of motion of the liquid in the photographs is vertically downward, which corresponds to the orientation of the experiment. The effect of gravity on present results, however, is negligible. Four shadowgraphs are shown in each case: one right at the jet exit which can be seen at the top of the photograph centered at $x/d_h = 2$, and the other three centered at $x/d_h = 8$, 18 and 28. A 2.4 mm diameter pin is visible at the left of each shadowgraph to

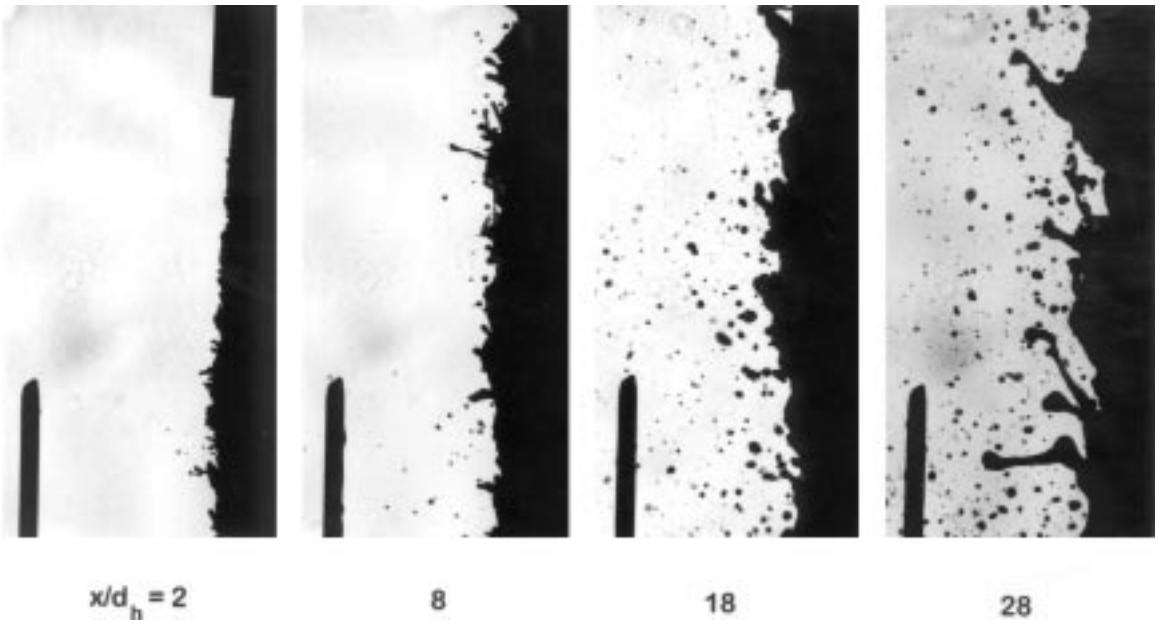

Fig. 1. Pulsed shadowgraphs at various positions along the surface of a plane turbulent free jet having a small velocity ($b = 6.75$ mm, $\overline{u}_0 = 15.8$ m/s, diameter of reference pin = 2.4 mm).

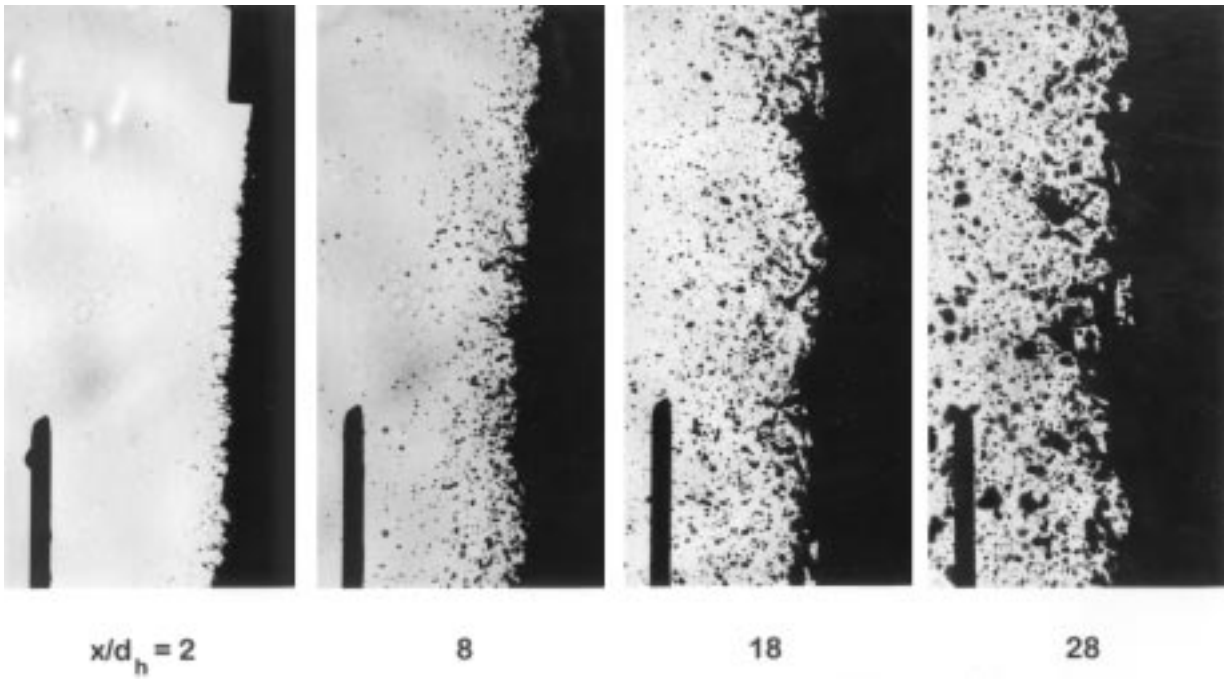

Fig. 2. Pulsed shadowgraphs at various positions along the surface of a plane turbulent free jet having a large velocity ($b = 6.75$ mm, $\bar{u}_0 = 28.2$ m/s, diameter of reference pin = 2.4 mm).

provide a distance reference. The outer surface of the liquid annulus, with the liquid core of the jet to the right, is pictured in all the shadowgraphs. When viewing these photographs it should be recalled that primary breakup, which yields the drops nearest to the liquid surface, is of interest here. Wider ranges of drop size, involving generally smaller drops, can be seen farther from the surface as a result of effects of secondary breakup.

The shadowgraphs of Figs. 1 and 2 illustrate a number of general features of the liquid surface during turbulent primary breakup. First of all, the liquid surface becomes rough, with protruding ligaments and other irregularities, relatively close to the jet exit. Subsequently, the diameter and length of the liquid surface roughness elements progressively increases with increasing distance from the jet exit. In addition, small scale disturbances are not even superimposed on the larger liquid structures that appear at far downstream locations. This behavior is qualitatively similar to past observations of turbulent primary breakup along round turbulent liquid jets in still gases (Ruff et al., 1991, 1992; Tseng et al., 1992; Wu et al., 1992; Wu and Faeth, 1993, 1995). Behavior along these lines is reasonable because small turbulent disturbances grow faster than large disturbances so that they should appear first, while the small levels of turbulence production in free liquid jets in gases at STP causes the turbulence to decay with the small scale portion of the turbulence spectrum disappearing first. The ligaments protruding from the liquid surface are randomly oriented rather than deflected toward the jet exit due to drag from the gas phase, which suggests small aerodynamic effects in agreement with earlier studies of round jets at similar liquid/gas density ratios (Wu et al., 1992; Wu and Faeth, 1993, 1995). Finally, the mean position of the liquid surface bulges outward near the jet

exit. It was demonstrated in several ways that these bulges were caused by adjustment of the flow from turbulent pipe flow conditions at the jet exit to nearly uniform mean velocity profiles in the free jets in air (due to small effects of aerodynamic drag on the liquid surface), rather than by effects of cavitation. First of all, earlier turbulence model predictions of flow structure, carried out in connection with the studies of Ruff et al. (1989, 1991) and Wu et al. (1992), exhibit similar bulges due to the changes of mean velocity profiles. Next, direct visualization of the liquid jets in the first and second wind-induced breakup regimes exhibit similar bulges, whereas the surface allows observations within the liquid which confirms the absence of bubbles in the flow (Ruff et al., 1989). In addition, observations of primary breakup near the onset of breakup, where ligaments are relatively sparse and the surface is smooth enough to see into the liquid, did not reveal the presence of any bubbles at these conditions. Finally, injection of liquids using supercavitating injectors at similar conditions yielded nonturbulent smooth round liquid jets with no bubbles within the liquid for observations extending hundreds of injector diameters (Wu et al., 1995).

The properties of drops formed by turbulent primary breakup, seen in Figs. 1 and 2, are also of interest. First of all, even though the liquid surface becomes roughened close to the jet exit, the first appearance of drops at the onset of turbulent primary breakup is deferred for a time. This occurs because the surface energy required to form very small drops is not available at the smallest scales of turbulence (Wu et al., 1992). After the onset of drop formation, however, drop diameters after turbulent primary breakup progressively increase with increasing distance from the jet exit, generally paralleling the corresponding increase of the scale of ligaments and other surface distortions. This behavior is consistent with drops separating from attached ligaments by a Rayleigh breakup process, i.e., that the ligaments act like liquid jets in the Rayleigh breakup regime as assumed during earlier approximate analysis of turbulent primary breakup of round liquid jets.

The effect of liquid velocity on liquid surface properties can be seen by comparing the shadowgraphs of Figs. 1 and 2. First of all, the length of the largest ligaments is seen to be relatively independent of liquid velocity. This behavior follows because turbulent eddy velocities scale with mean streamwise velocities for turbulent flow. Then, increasing mean streamwise velocities increases cross stream velocities at the same rate so that distances traveled in the cross stream direction when a given streamwise position is reached remain the same. In contrast, the smallest scale disturbances become progressively smaller as the streamwise liquid velocity increases because the kinetic energy available to distort the surface at large wave numbers increases as the velocity and, thus, the Reynolds number of the flow increases. The net effect is similar to turbulent jet mixing where increasing jet velocities (Reynolds numbers) do not affect the global mixing process of the flow even though fine scale mixing is increased (Schlichting, 1979; Hinze, 1975; Tennekes and Lumley, 1972).

The effects of liquid velocity on the properties of drops formed by turbulent primary breakup, seen in Figs. 1 and 2, are generally related to the properties of the distortion of the liquid surface. Thus, larger velocities increase turbulence energies at small scales which implies that smaller drops can form at the onset of turbulent primary breakup, which correspondingly occurs at smaller distances from the jet exit. In addition, drop sizes resulting from turbulent primary breakup at a particular streamwise position tend to decrease as liquid velocities increase, more or less proportional to the variation of ligament size. This causes an increase in

the drop number density near the surface with increasing velocity because drop diameters decrease and the ligament density increases. Measurements of liquid volume fractions near the liquid surface for turbulent primary breakup of round liquid jets, however, suggest that they are not correspondingly influenced by the liquid jet velocity (Ruff et al., 1992; Tseng et al., 1992). Such behavior is typical of turbulent mixing because variations of scalar concentrations as a function of distance from the jet exit do not change rapidly as the jet velocity changes.

3.2. Liquid surface velocities

Present measurements of streamwise mean liquid surface velocities, $\overline{u}_s$, are reported by Dai et al. (1998b) and will be discussed only briefly. Surface velocities are small near the jet exit due to the retarding effect of the jet passage wall. Surface velocities increase rapidly in the streamwise direction, however, $\overline{u}_s \approx \overline{u}_0$ (within 10%) for $50 < x/\Lambda < 800$, where Λ is the radial integral length scale and $x/\Lambda = 800$ is the largest distance from the jet exit considered during the present investigation. Similar to past work, e.g., Dai et al. (1998a, 1998b) and references cited therein, the streamwise integral length scale was taken to be 4Λ, where $\Lambda = d_h/8$, based on Laufer's measurements of the properties of fully-developed turbulent pipe flow, see Hinze (1975) and references cited therein. The fact that $\overline{u}_s \approx \overline{u}_0$, for most of the present flow, agrees with earlier observations of surface velocities for round jets (Wu et al., 1995). In contrast, plane turbulent wall jets exhibit a significant reduction of surface velocities for similar streamwise distances (Dai et al., 1997, 1998a). These differences highlight the relatively weak effects of aerodynamic drag at the gas/liquid interface for free jets when liquid/gas density ratios are large, compared to the solid surface of a plane turbulent wall jet.

3.3. Drop size distributions

Drop size distributions were not measured during the present investigation. Past work, however, has shown good agreement between the universal root normal distribution function of Simmons (1977) and measured drop size distribution functions for a variety of primary and secondary breakup processes (Hsiang and Faeth, 1992, 1993; Ruff et al., 1992; Tseng et al., 1992; Wu et al., 1992; Wu and Faeth, 1993, 1995). Thus, this distribution function will be assumed to be appropriate for present measurements. The universal root normal distribution function is defined by MMD/SMD = 1.2, where MMD is the mass medium drop diameter of the spray. As a result, specification of one more moment of this two-moment function completely prescribes drop size properties; this additional moment will be taken to be the SMD in the following section.

3.4. Drop velocity distributions

Typical distributions of drop velocity as a function of drop size after turbulent primary breakup are illustrated in Figs. 3 and 4. Mean values of streamwise and cross stream velocities, u and v, for a particular drop diameter, d, are plotted as a function of drop diameter in Fig. 3 for a variety test conditions. The velocities in this plot are normalized by the mass-weighted (Favre) averaged velocities, $\tilde{u}$ and $\tilde{v}$, while the drop diameters are normalized by the SMD, at

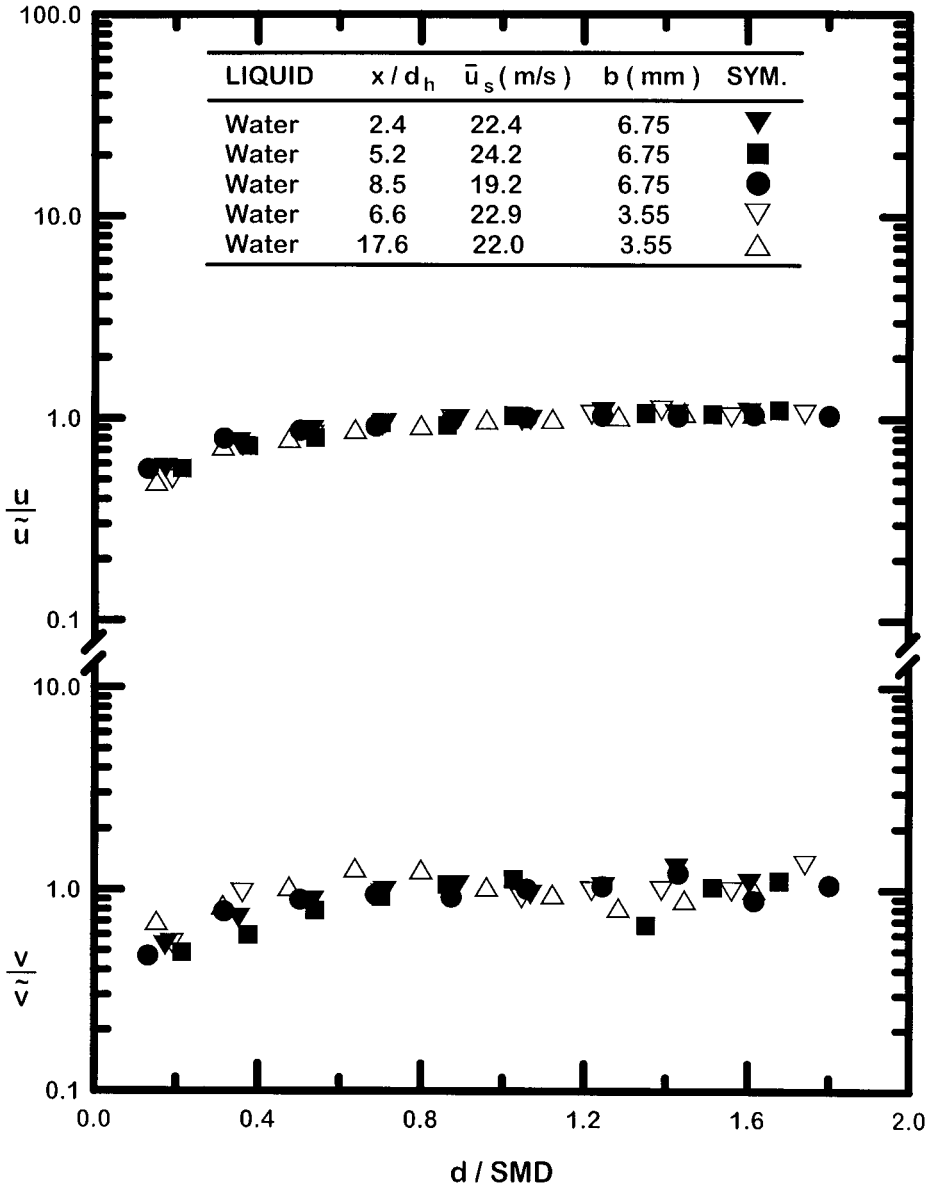

Fig. 3. Distributions of mean streamwise and cross stream velocities after turbulent primary breakup as a function of drop size.

each test condition. The values of both $u/\tilde{u}$ and $v/\tilde{v}$ are seen to increase in magnitude with increasing d/SMD initially, but then remain nearly unity (within experimental uncertainties) for $0.3<d/\mathrm{SMD}$. Consideration of the behavior of the small drops, however, suggest that their velocities tend to be smaller than the rest due to their rapid relaxation toward the local gas velocity. In addition, the effect of small drops on the momentum exchange between the phases is not very important because they have correspondingly small inertias. Thus, assuming

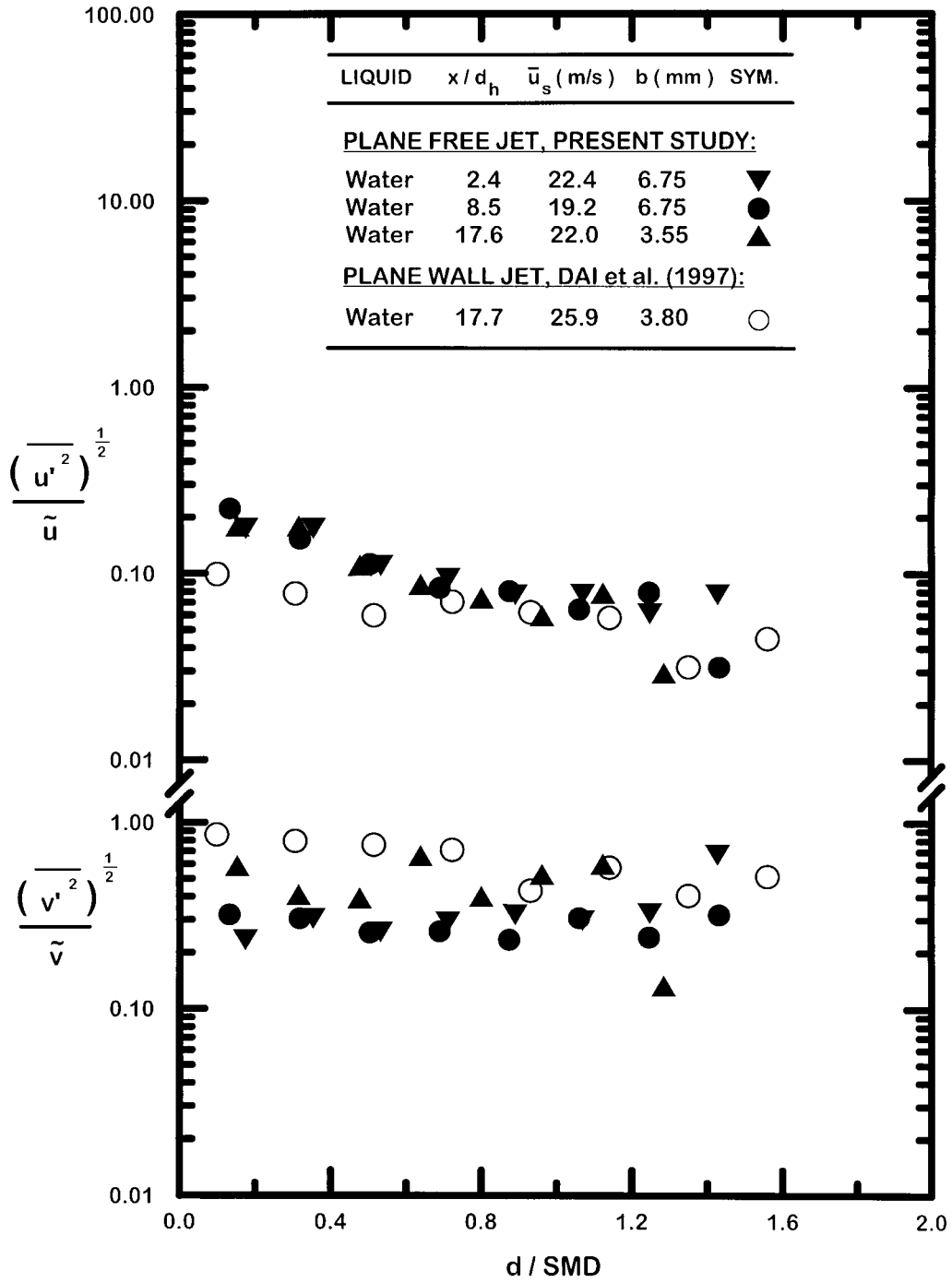

Fig. 4. Distributions of rms fluctuating streamwise and cross stream velocities after turbulent primary breakup as a function of drop size.

uniform drop velocity distributions after turbulent primary breakup at each point along the surface appears to be justified based on the present measurements. Similar conclusions were obtained from analysis of earlier drop velocity measurements after turbulent primary breakup for wall jets due to Dai et al. (1997).

Fig. 4 is an illustration of rms streamwise and cross stream drop velocity fluctuations, $\overline{u}'$ and $\overline{v}'$, as a function of normalized drop diameter, d/SMD, for a variety of test conditions. Results for plane wall jets due to Dai et al. (1997) are also shown in the plots for comparison with the present measurements. Results at various test conditions tend to scatter at each normalized drop size, however, this behavior is felt to be mainly due to the relatively large experimental uncertainties of these velocities. The tendency for drop velocity fluctuations to increase as drop sizes become small may be due to the effects of relaxation of the motion of small drops as discussed in connection with Fig. 3. Thus, it is concluded that drop velocity fluctuations after turbulent primary breakup are represented reasonably well by uniform distribution functions with respect to drop size, similar to mean velocities.

3.5. Mean and fluctuating drop velocities

Favre-averaged mean streamwise and cross stream velocities after turbulent primary breakup are plotted as a function of distance from the jet exit in Fig. 5, for various test conditions. The normalized distance variable used in this figure is $x/(\Lambda We_{L\Lambda}^{0.5})$ where $We_{L\Lambda} = \rho_L \overline{u}_0^2 \Lambda/\sigma$. This streamwise distance variable was chosen for consistency, with drop size results to be considered later. The findings for drop sizes will suggest that the end of the all-liquid core is approached when the normalized streamwise distance variable used in Fig. 5 has values on the order of 10; this condition is approached by present velocity measurements farthest from the jet exit. The measurements of Dai et al. (1997) for plane wall jets are also shown in the plots for comparison with the present measurements.

Results plotted in Fig. 5 show that mean streamwise velocities are roughly equal to local streamwise liquid surface velocities for both wall jets and free jets. For present results, since $\overline{u}_s \approx \overline{u}_0$ over much of the test range, streamwise velocities of drops after turbulent primary breakup are approximated rather well by the mean streamwise jet exit velocity. Present mean cross stream velocities, however, behave rather differently from streamwise velocities: cross stream velocities decrease with increasing streamwise distance, and they are not in good agreement with past measurements for wall jets. The present variation of $\tilde{v}$ with streamwise distance, however, is quite plausible. Near the jet exit, $\tilde{v}$ for free jets is larger than for wall jets because cross stream flapping of the liquid core is not constrained by the wall for free jets. In contrast, as the end of the all liquid core is approached for the free jets, the mean cross stream velocity should become small due to symmetry, i.e., cross stream motion in either direction is equally probable when the end of the liquid core is reached. The presence of the wall, however, only allows cross stream motion away from the liquid surface so that $\tilde{v}/\overline{u}_s$ tends to remain constant for wall jets.

Favre-averaged fluctuating streamwise and cross stream velocity fluctuations are plotted as a function of normalized streamwise distance in Fig. 6. As before, results from Dai et al. (1997) for plane wall jets are also plotted in the figure for comparison with the present measurements. All these results are relatively independent of distance from the jet exit.

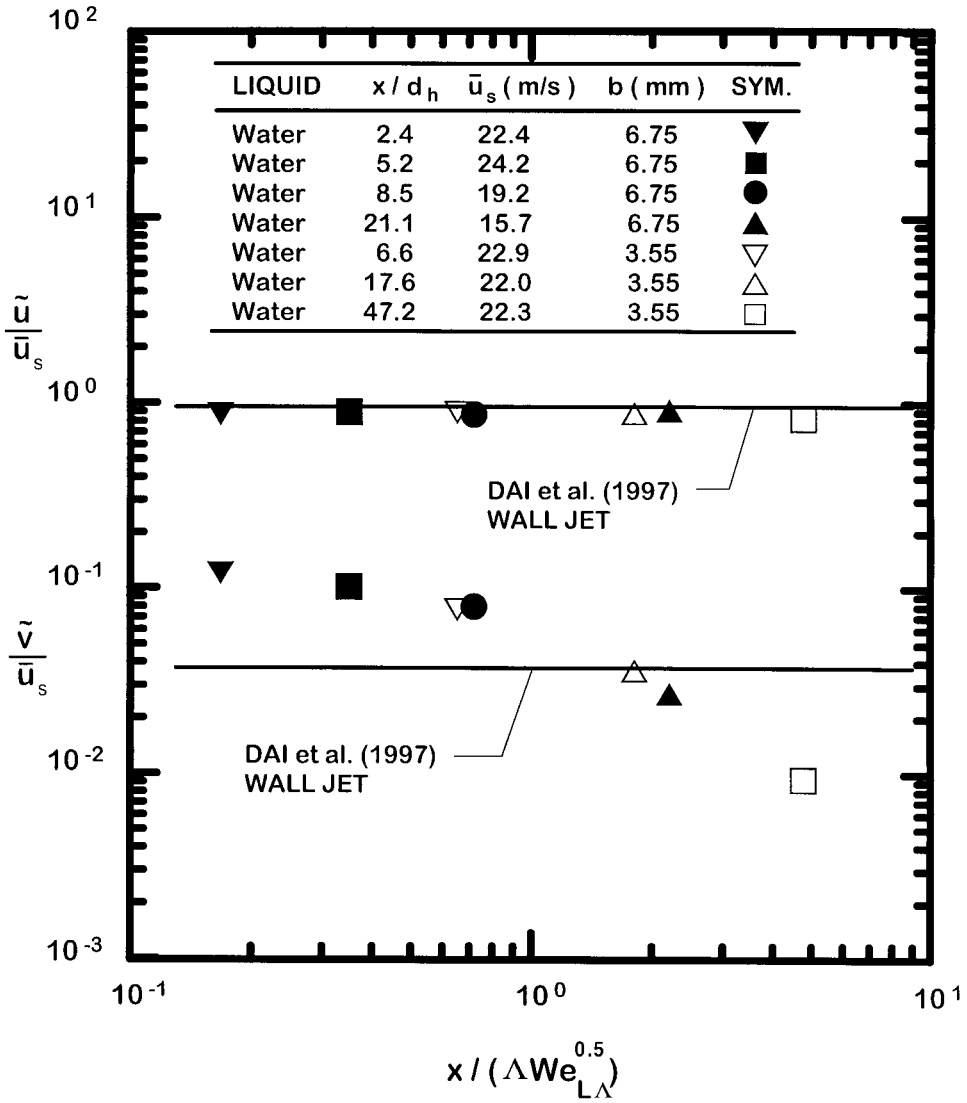

Fig. 5. Mean streamwise and cross stream velocities after turbulent primary breakup as a function of distance along the surface of plane free jets.

3.6. Onset of breakup

The properties of the onset of turbulent primary breakup for plane free jets were analyzed in the same manner as earlier studies of round free jets and plane wall jets, see Wu and Faeth (1995), Dai et al. (1997, 1998a) and references cited therein for complete details. Drop sizes at the onset of turbulent primary breakup were found by equating the kinetic energy (relative to its surroundings) of a characteristic eddy of a given size to the surface energy required to form a drop of corresponding size. Drop and eddy sizes were assumed to be in the inertial range of the turbulence which was appropriate for present test conditions, see Wu and Faeth (1995) for

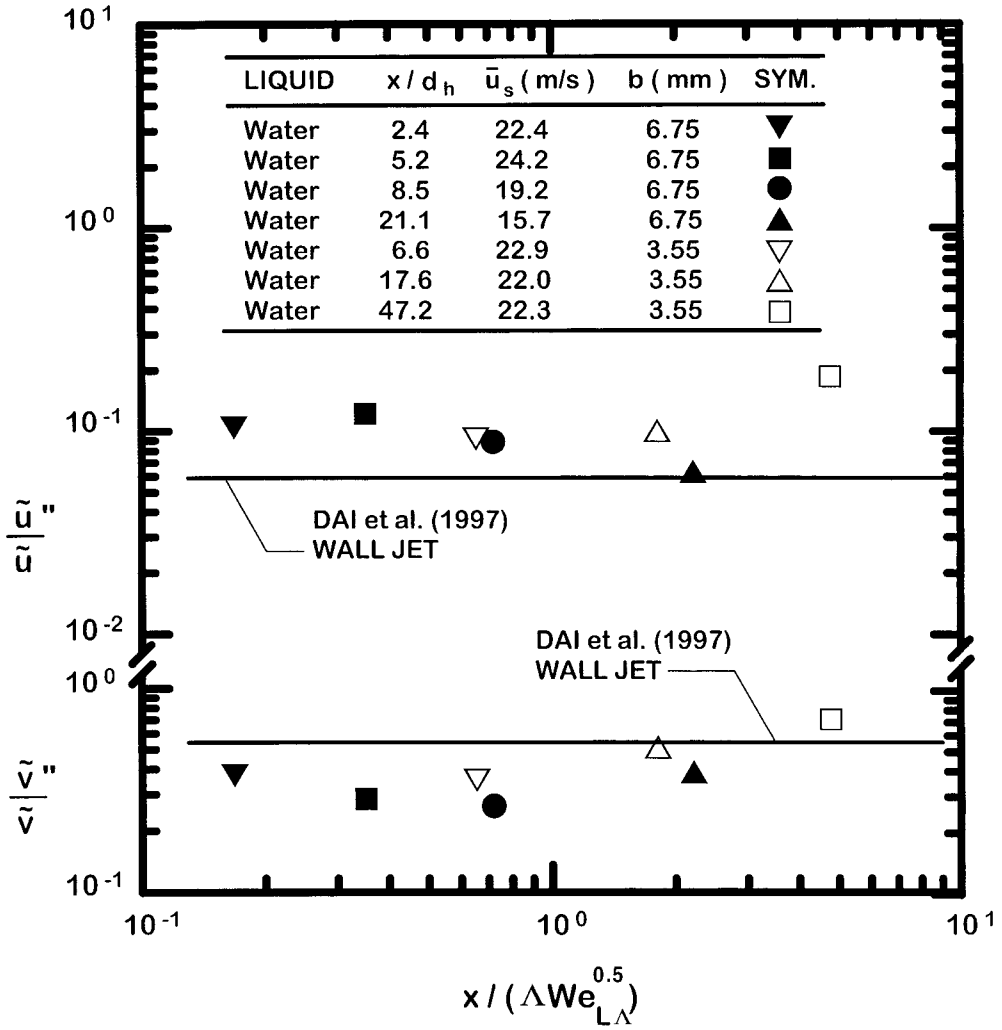

Fig. 6. Fluctuating streamwise and cross stream velocities after turbulent primary breakup as a function of distance along the surface of plane free jets.

consideration of turbulent primary breakup for eddy sizes outside the inertial range. Within the inertial range, eddy sizes and velocities are related in a simple way as discussed by Tennekes and Lumley (1972). Finally, the SMD resulting from turbulent primary breakup was associated with the characteristic eddy size to yield the following expression for the SMD at the onset of turbulent primary breakup

$$\frac{\mathrm{SMD}_i}{\Lambda} = C_{si}\left(\frac{\overline{u}_0}{\overline{v}_0'}\right)^{6/5} We_{L\Lambda}^{-3/5} \tag{1}$$

where $\overline{v}_0'$ is the average cross stream velocity fluctuation at the jet exit and C_{si} is an empirical constant on the order of unity involving various constants of proportionality. Given that $\overline{v}_0'/\overline{u}_0$

is a constant for fully-developed turbulent pipe flow, SMD_i/Λ should be only a function of $We_{L\Lambda}$ for present test conditions.

Present measurements of SMD_i are plotted as suggested by Eq. (1) in Fig. 7, along with the measurements and correlation of Wu and Faeth (1993) for round free jets and the correlation of Dai et al. (1997) for plane wall jets. The results for the round and plane free jets are in excellent agreement showing that the hydraulic diameter correctly represents the effects of the different configurations of these two flows. The best-fit correlation of both sets of measurements is as follows:

$$\frac{SMD_i}{\Lambda} = 134 We_{L\Lambda}^{-0.76} \tag{2}$$

The standard deviation of the coefficient and power of Eq. (2) are 7 and 5%, respectively, and the correlation coefficient of the fit is 0.97. This expression is very close to the earlier correlation for round jets of Wu and Faeth (1993). The reduction of the power of $We_{L\Lambda}$ from

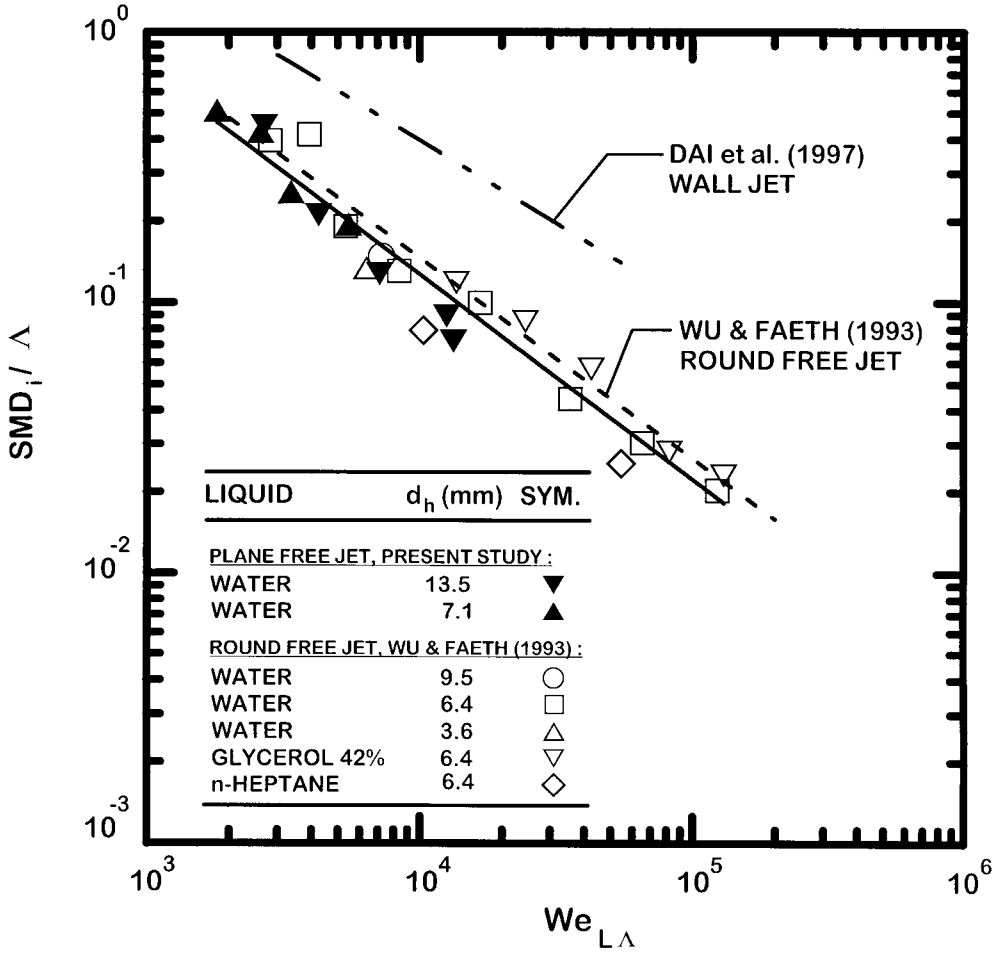

Fig. 7. SMD at the onset of turbulent primary breakup as a function of Weber number for plane free jets.

−0.60 in Eq. (1) to −0.76 in Eq. (2) is statistically significant, but is not large in view of the approximations used to find Eq. (1) and experimental uncertainties. The coefficient of Eq. (2) is large but this is expected because $(\overline{u}_0/\overline{v}_0')^{6/5}$ is large; therefore, C_{si} is on the order of unity as expected. The correlation of Dai et al. (1997) for plane wall jets yields values of SMD_i that are larger than the values for the free jets. Such differences are not unreasonable, however, because free jets are slowly decaying flows with turbulence properties dominated by near solid surface conditions at the onset of turbulent primary breakup, whereas wall jets are developing flows with turbulence properties dominated by conditions far from the solid surface at the onset of turbulent breakup.

An expression for the location of the onset of turbulent primary breakup was developed, following methods used earlier for round free jets and plane wall jets. It was assumed that the drop-forming eddy convects along the surface at a streamwise velocity $\overline{u}_0$ for the time required for an eddy of characteristic size to form a drop. The breakup time was taken to be the time required for Rayleigh breakup of a ligament having a diameter equal to the diameter of the characteristic eddy from Weber (1931), while ignoring a viscous term that might become important at large jet Ohnesorge numbers. Thus, fixing the value of SMD_i from Eq. (1) yields the following expression for the location of the onset of breakup:

$$\frac{x_i}{\Lambda} = C_{xi}\left(\frac{\overline{u}_0}{\overline{v}_0'}\right)^{9/5} We_{L\Lambda}^{-0.4} \tag{3}$$

where C_{xi} is an empirical parameter on the order of unity, involving the various constants of proportionality.

Present measurements of x_i are plotted as suggested by Eq. (3) in Fig. 8, along with the measurements and correlation of Wu and Faeth (1993) for round free jets and the correlation of Dai et al. (1997) for plane wall jets. The results for the round and plane free jets are in excellent agreement which also shows that the hydraulic diameter represents effects of the different configurations of these two flows. The best-fit correlation of both sets of measurements is as follows:

$$\frac{x_i}{\Lambda} = 7560\, We_{L\Lambda}^{-0.74} \tag{4}$$

The standard deviation of the coefficient and power of Eq. (4) are 7 and 9%, respectively, and the correlation coefficient of the fit is 0.91. This expression is very close to the earlier correlation for round jets of Wu and Faeth (1993). As before, the power of $We_{L\Lambda}$ in Eq. (4) is not −0.4 as suggested by Eq. (3), but the differences are not large in view of the approximations used to find Eq. (3) and the relatively large experimental uncertainties of the measurements. Finally, the large value of the constant in Eq. (4) can be expected because $(\overline{u}_0/\overline{v}_0')^{9/5}$ is large in Eq. (3), yielding a value of C_{xi} on the order of unity.

3.7. Drop sizes along surface

An expression for the variation of the SMD with distance from the jet exit was developed, following methods used earlier for round free jets and plane wall jets. It was assumed that the

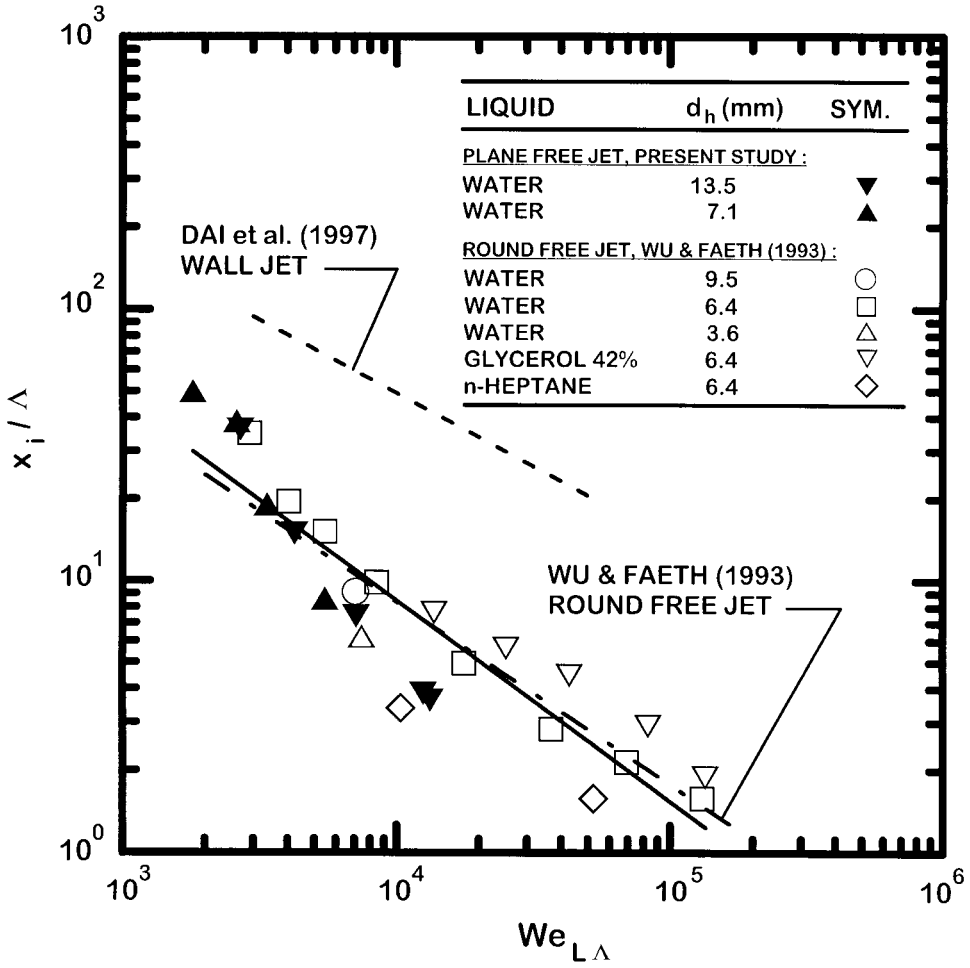

Fig. 8. Length to initiate turbulent primary breakup as a function of distance along the surface as a function of Weber number for plane free jets.

SMD is dominated by the largest drop that can be formed at a particular position, that an eddy of this characteristic size forms a drop by Rayleigh breakup, that effects of liquid viscosity on breakup are small, and that the SMD is proportional to the characteristic eddy size. Then, proceeding similar to Eq. (3), the following expression for the variation of SMD with distance from the jet exit is obtained:

$$\frac{\mathrm{SMD}}{\Lambda} = C_{sx}\left(\frac{x}{\Lambda We_{L\Lambda}^{1/2}}\right)^{2/3} \tag{5}$$

where C_{sx} is an empirical parameter on the order of unity.

Present measurements of SMD are plotted as suggested by Eq. (5) in Fig. 9, along with the correlations of Wu et al. (1995) for round free jets and Dai et al. (1997) for plane wall jets. In this case, results for all three flows agree within experimental uncertainties with the best-fit

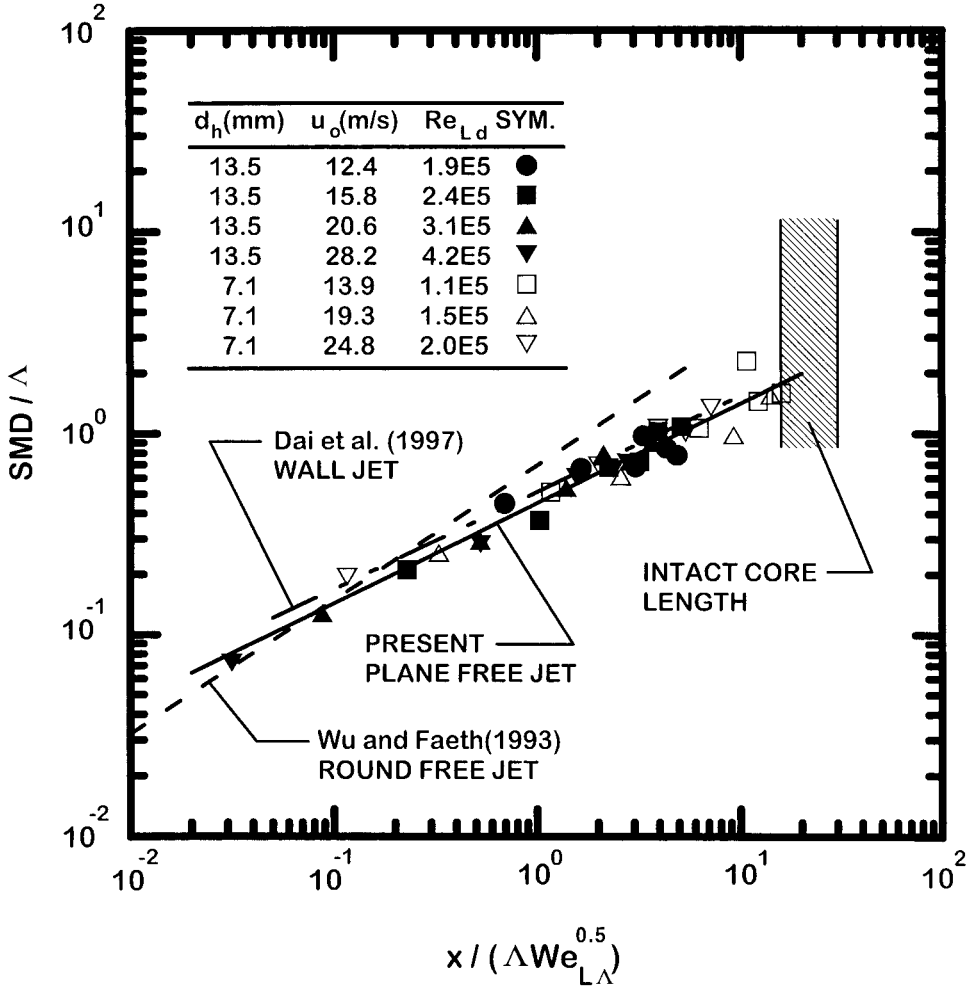

Fig. 9. SMD after turbulent primary breakup as a function of distance along the surface of the plane free jets.

correlation of the present measurements as follows:

$$\frac{\mathrm{SMD}}{\Lambda} = 0.45\left(\frac{x}{\Lambda We_{L\Lambda}^{1/2}}\right)^{0.5} \tag{6}$$

The standard deviations of the coefficient and power of Eq. (6) are 10 and 6%, respectively, and the correlation coefficient of the fit is 0.98. The power of the normalized streamwise distance variable in Eq. (6) is not 0.67 as suggested by Eq. (5), but the difference is not large in view of the approximations used to find (5) and experimental uncertainties. Finally, the coefficient of Eq. (6) is properly on the order of unity because there is no term proportional to a power of $\overline{u}_0/\overline{v}_0'$ present in this case to generate a large value for this coefficient. Taken together, the reasonable values of the empirical coefficients and powers of Eqs. (2), (4) and (6),

and the large correlation coefficients of the fits, help to support the physical ideas used to develop these expressions.

Based on Eq. (6), increasing streamwise distance will eventually yield a condition where the SMD becomes comparable to the cross stream dimension of the free jet or wall jet. At such conditions, it is expected that SMD/Λ should be on the order of unity. It is interesting to note that this condition roughly corresponds to the end of the intact liquid core (or jet breakup length) of round free jets reported by Grant and Middleman (1966) as plotted in Fig. 9 (note that this correlation appears as a band over the present test range as discussed by Wu et al. (1992). Use of hydraulic diameters to treat other geometries suggests similar liquid column breakup lengths for round and plane free jets and plane wall jets, but this behavior has not yet been established by experiments.

4. Conclusions

The velocities of the liquid surface, and drop velocities and sizes after turbulent primary breakup along the liquid surface, were measured for plane turbulent water jets in still air at STP. Test conditions included $\rho_L/\rho_G \approx 860$, $Re_{Ld} = 91{,}000 - 424{,}000$, $We_{Ld} = 13{,}000 - 151{,}000$ and $Oh_{Ld} = 0.0009 - 0.0012$, the last implying conditions where direct effects of liquid viscosity are small. The major conclusions of the study are as follows:

1. Liquid surface roughness and drop formation along the liquid surface were caused by liquid turbulence developed within the injector passage, whereas direct aerodynamic effects were small for present test conditions.
2. Streamwise liquid surface velocities were nearly constant (within 10%) over most of the liquid surface ($50 < x/\Lambda < 800$) due to ineffective aerodynamic forces, however, surface velocities were smaller near the jet exit due to the retarding effect of the jet passage walls.
3. Drop velocity distributions after turbulent primary breakup satisfied uniform distribution functions; this is helpful because velocities are fully defined by single moments.
4. Mean and fluctuating drop velocities after turbulent primary breakup could be related quite simply to mean streamwise velocities in the liquid. Velocity properties were similar to recent observations of plane wall jets except for mean cross stream velocities, which decrease with increasing streamwise distance rather than remaining constant similar to wall jets.
5. The use of hydraulic diameter concepts yielded correlations for the SMD and location at the onset of turbulent primary breakup, and for the variation of SMD after turbulent primary breakup as a function of distance along the surface, that are identical (within experimental uncertainties) for round and plane free turbulent jets in still gases. In contrast, the onset of turbulent primary breakup for plane wall jets is deferred to larger drop sizes and distances from the jet exit compared to the free jets, although the variation of SMD with distance along the surface is similar for all three flows. It is thought that the different onset properties come about because onset involves small turbulence scales near surfaces for free jets as opposed to large turbulence scales far from surfaces for wall jets.

Present observations are limited to liquids having moderate viscosities and fully developed liquid turbulence, where drop sizes after breakup are comparable to eddy sizes in the inertial

range of turbulence, where liquid surface breakup is not too near conditions where the entire liquid sheet breaks up, and where aerodynamic effects on turbulent primary breakup are not important. Addressing these limitations clearly merits more attention.

Acknowledgements

This research was supported by the Office of Naval Research, Grant No. N00014-95-1-0234 under the technical management of E.P. Rood. Initial development of research facilities for this study was carried out under Air Force Office of Scientific Research Grant No. AFOSR F49620-95-1-0364 under the technical management of J.M. Tishkoff.

References

Dai, Z., Hsiang, L.-P., Faeth, G.M., 1997. Spray formation at the free surface of turbulent bow sheets. In: Proceedings of the Twenty-First Symposium on Naval Hydrodynamics. National Academy Press, Washington, DC, 490–505.

Dai, Z., Chou, W.-H., Faeth, G.M., 1998a. Drop formation due to turbulent primary breakup at the free surface of plane liquid wall jets. Phys. Fluids 10, 1147–1157.

Dai, Z., Sallam, K.A., Faeth, G.M., 1998b. Turbulent primary drop breakup from plane-free bow sheets. In: Proceedings of the Twenty-Second Symposium on Naval Hydrodynamics. National Academy Press, Washington, DC.

de Juhasz, K.J., Zahn, O.F., Jr., Schweitzer, P.H., 1932. On the formation and dispersion of oil sprays. Bulletin No. 40, Engineering Experiment Station, Pennsylvania State University, University Park, PA.

Ervine, D.A., Falvey, H.T., 1987. Behavior of turbulent water jets in the atmosphere and in plunge pools. Proc. Inst. Civ. Eng. (Part 2) 83, 295–314.

Gad-el-Hak, M., 1981. Measurements of turbulence and wave statistics in wind-waves. In: International Symposium on Hydrodynamics in Ocean Engineering. The Norwegian Institute of Technology, Oslo, 403–417.

Grant, R.P., Middleman, S., 1966. Newtonian jet stability. AIChE J. 12, 669–678.

Hinze, J.O., 1975. Turbulence, 2nd ed. McGraw-Hill, New York, pp. 427, 724–734.

Hoyt, J.W., Taylor, J.J., 1977a. Waves on water jets. J. Fluid Mech. 88, 119–123.

Hoyt, J.W., Taylor, J.J., 1977b. Turbulence structure in a water jet discharging in air. Phys. Fluids 20, S253–S257.

Hsiang, L.-P., Faeth, G.M., 1992. Near-limit drop deformation and secondary breakup. Int. J. Multiphase Flow 18, 635–652.

Hsiang, L.-P., Faeth, G.M., 1993. Drop properties after secondary breakup. Int. J. Multiphase Flow 19, 721–735.

Lee, D.W., Spencer, R.C., 1933. Preliminary photomicrographic studies of fuel sprays. NACA Tech. Note 424, Washington.

Lee, D.W., Spencer, R.C., 1933. Photomicrographic studies of fuel sprays. NACA Tech. Note 454, Washington.

McCarthy, M.J., Malloy, N.A., 1974. Review of stability of liquid jets and the influence of nozzle design. Chem. Eng. J 7, 1–20.

Phinney, R.E., 1973. The breakup of a turbulent jet in a gaseous atmosphere. J. Fluid Mech. 60, 689–701.

Ruff, G.A., Sagar, A.M., Faeth, G.M., 1989. Stucture and mixing properties of pressure-atomized sprays. AIAA J. 27, 901–908.

Ruff, G.A., Bernal, L.P., Faeth, G.M., 1991. Structure of the near injector region of non-evaporating pressure-atomized sprays. J. Prop. Power 7, 221–230.

Ruff, G.A., Wu, P.-K., Bernal, L.P., Faeth, G.M., 1992. Continuous- and dispersed-phase structure of dense non-evaporating pressure-atomized sprays. J. Prop. Power 8, 280–289.

Schlichting, H., 1979. Boundary Layer Theory, 7th ed. McGraw-Hill, New York, p. 599.
Schweitzer, P.H., 1937. Mechanism of disintegration of liquid jets. J. Appl. Phys. 8, 513–521.
Simmons, H.C., 1977. The correlation of drop-size distributions in fuel nozzle sprays. J. Eng. Power 99, 309–319.
Tennekes, H., Lumley, J.L., 1972. A First Course in Turbulence. MIT Press, Cambridge, MA, pp. 248–286.
Townson, J.M., 1988. Free-Surface Hydraulics, 1st ed. Unwin Hyman, London, Chapter 6.
Tseng, L.-K., Ruff, G.A., Faeth, G.M., 1992. Effects of gas density on the structure of liquid jets in still gases. AIAA J. 30, 1537–1544.
Weber, C., 1931. Zum zerfall eines flussigkeitsstrahles. Z. Angewesen. Math. Mech. 2, 136–141.
Wu, P.-K., Faeth, G.M., 1993. Aerodynamic effects on primary breakup of turbulent liquids. Atom. Sprays 3, 265–289.
Wu, P.-K., Faeth, G.M., 1995. Onset and end of drop formation along the surface of turbulent liquid jets in still gases. Phys. Fluids A7, 2915–2917.
Wu, P.-K., Tseng, L.-K., Faeth, G.M., 1992. Primary breakup in gas/liquid mixing layers for turbulent liquids. Atom. Sprays 2, 295–317.
Wu, P.-K., Miranda, R.F., Faeth, G.M., 1995. Effects of initial flow conditions on primary breakup of nonturbulent and turbulent round liquid jets. Atom. Sprays 5, 175–196.